International Journal of Medical, Medicine and Health Sciences
ISSN: 2517-9969
Vol:11, No:6, 2017

An Inverse Heat Transfer Algorithm for Predicting the Thermal Properties of Tumors during Cryosurgery

Mohamed Hafid, Marcel Lacroix

***Abstract*—**This study aimed at developing an inverse heat transfer approach for predicting the time-varying freezing front and the temperature distribution of tumors during cryosurgery. Using a temperature probe pressed against the layer of tumor, the inverse approach is able to predict simultaneously the metabolic heat generation and the blood perfusion rate of the tumor. Once these parameters are predicted, the temperature-field and time-varying freezing fronts are determined with the direct model. The direct model rests on one-dimensional *Pennes* bioheat equation. The phase change problem is handled with the enthalpy method. The *Levenberg-Marquardt* Method (LMM) combined to the *Broyden* Method (BM) is used to solve the inverse model. The effect (a) of the thermal properties of the diseased tissues; (b) of the initial guesses for the unknown thermal properties; (c) of the data capture frequency; and (d) of the noise on the recorded temperatures is examined. It is shown that the proposed inverse approach remains accurate for all the cases investigated.

***Keywords*—**Cryosurgery, inverse heat transfer, *Levenberg-Marquardt* method, thermal properties, *Pennes* model, enthalpy method.

I. Introduction

CRYOSURGERY has become a well-established technique for the ablation of undesirable tissues such as tumors and cancers. It is an effective treatment for external tumors such as ear tumors and skin tumors, and for internal tumors such as lung tumors and breast tumors. Cryosurgery is often preferred to the traditional surgery due to the fact that it is minimally invasive and the hospitalization time is reduced.

Cryosurgery resorts to extreme cold for destroying diseased tissues. It works by taking advantage of the destructive effect of freezing temperatures on living cells. The instrument used to freeze the tissues is a cryoprobe. The low temperatures are obtained by circulating liquid nitrogen through the cryoprobe.

As illustrated in Fig. 1, the cryoprobe is inserted in such a way as to optimize the freezing of the tumor. When the rate of cooling is very high, ice crystals form inside the cells. These ice crystals damage the cell membrane and lead to the destruction of the tumor. Furthermore, the formation of ice crystals harms the blood vessels that supply the tumor tissue.

Destroying the diseased tissues while minimizing the damages to the surrounding healthy tissues is however a challenging task. Sophisticated imaging techniques such as Magnetic Resonance Imaging (MRI) or ultrasounds must be used to guide the cryoprobe and monitor the freezing of the cells [1], [2]. But, these imaging techniques are often unavailable. Moreover, they cannot reproduce the time-varying temperature distribution inside the layer of tissue.

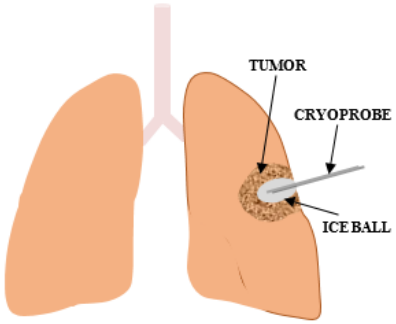

Fig. 1 Cryosurgery of lung tumor

An alternative to MRI or ultrasounds is the mathematical modeling of the heat transfer and the freezing processes that take place inside the tissues [3]-[6]. But, in order to perform the mathematical analysis, the thermal properties of the tissues, such as the metabolic heat generation and the blood perfusion, must be known. Measuring these properties with experimental techniques is however a complicated task [7], [8]. They require sophisticated equipment that can hardly be employed during cryosurgery. This is where inverse heat transfer methods come to the rescue [9]. In these methods, the unknown thermal properties may be determined by means of temperatures recorded by a temperature probe pressed against the layer of tissue.

Many studies based on inverse methods have been carried out in the past for predicting the blood perfusion coefficient [10], the unknown time-dependent surface heat flux in a living skin tissue [11], and the size and the location of the tumor [12]-[16]. Studies also focused on the simultaneous estimation of various other thermo-physical properties using inverse approach [17]-[21].

In all the aforementioned investigations however, the prediction of the thermal properties of the biological tissues during cryosurgery was not carried out.

The main purpose of the present paper is to pursue the aforementioned studies by developing an inverse method capable of estimating the unknown metabolic heat generation rate and the blood perfusion rate during cryosurgery. Once these unknown parameters are determined, the temperature-

Hafid M. is with the Department of Mechanical Engineering, Université de Sherbrooke, 2500 Blvd. de l'Université, Sherbrooke (Québec) J1K 2R1, Canada (corresponding author, phone: (873) 888-7768, e-mail: mohamed.hafid@usherbrooke.ca).
Lacroix M. is with the Department of Mechanical Engineering, Université de Sherbrooke, 2500 Blvd. de l'Université, Sherbrooke (Québec) J1K 2R1, Canada (phone: (819)821-8000 poste 62145, e-mail: Marcel.Lacroix@uSherbrooke.ca).

field and the moving freezing front are predicted. Overall, the proposed method may become, one day, a viable alternative to more expensive imaging techniques that are used in cryosurgery.

This paper is organized as follows. First, a one-dimensional finite-volume model based on the *Pennes* bioheat equation and the non-isothermal phase change enthalpy method is developed. The model is then validated with an analytical solution available in the open literature. Second, an inverse procedure based on the *Levenberg-Marquardt* Method (LMM) combined to the *Broyden* Method (BM) is presented. Finally, the proposed inverse procedure is thoroughly tested for several freezing scenarios.

II. Problem Statement and Assumptions

Fig. 2 illustrates the one-dimensional phase change problem for cryosurgery. Three regions are considered: (1) the frozen zone whose time-varying interface position is *s(t)*, (2) the mushy zone and (3) the intact (unfrozen) zone. The lower and upper phase change interfaces are defined as the distance that separates the cryoprobe from the solidus temperature T_{sol} and the liquidus temperature T_{liq}, respectively. A freezing temperature T_c, which represents the temperature of the cryoprobe, is imposed on the left boundary condition (at $x = 0$). At the right boundary ($x=L_t$), the temperature gradient is set equal to zero. No heat is transferred as this boundary is far removed from the cryoprobe. The thickness of the tissue is set equal to L_t=0.05 m.

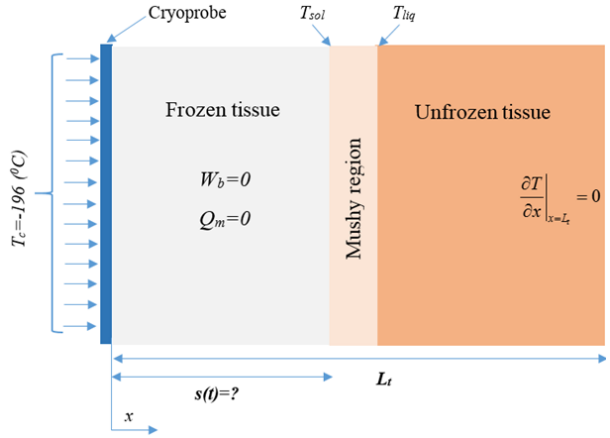

Fig. 2 One-dimensional problem of cryosurgery

The mathematical model of cryosurgery rests on the following assumptions:

- Heat is predominantly transferred from the tissue to the cryoprobe. Thus, a one-dimensional heat transfer model can be applied [22].
- The blood perfusion rate and the metabolic heat generation are assumed to be uniform through time and space.
- The blood perfusion rate and the metabolic heat generation are set equal to zero in the frozen and in the mushy regions.
- The blood temperature is set equal to T_b=37 °C.
- The phase change of the diseased tissue is non-isothermal. The freezing process is characterized by three zones: a frozen solid zone, a mushy zone, and an unfrozen zone (Fig. 2).
- The liquidus temperature T_{liq} (the upper limit) and the solidus temperature T_{sol} (the lower limit) of the biological tissue are set equal to -1 °C and -8 °C, respectively [23], [24].
- The heat transfer inside the diseased tissue is conduction dominated [25], [26].
- The effect of large blood vessels is neglected [27], [28].

III. The Direct Problem

For the direct problem, all the thermo-physical properties, the initial and the boundary conditions are known. The mathematical model for the heat transfer inside the biological tissue is given by the fundamental *Pennes* bio-heat equation [29]:

$$\rho c\frac{\partial T}{\partial t}=\frac{\partial}{\partial x}\left(k\frac{\partial T}{\partial x}\right)+\rho_b c_b w_b\left(T_b-T\right)+Q_m+\delta H\frac{\partial f_s}{\partial t} \tag{1}$$

ρ, c, and k are the density, the specific heat, and the thermal conductivity of the tissue, respectively. The subscript 'b' refers to the blood characteristics. w_b and Q_m represent the blood perfusion rate and the metabolic heat generation in the tissue, respectively. T is the tissue temperature, and T_b is the arterial blood temperature.

The last term on the right-hand side of (1) represents the liquid/solid phase change of the tissue during cryosurgery. δH and f_s are the enthalpy and the solid fraction during the phase change, respectively. The enthalpy δH is defined as $\delta H=\rho(c_{solid}-c_{liquid})T-\rho\lambda$, and the solid fraction may be expressed as

$$f_s=F\left(T\right)=\begin{cases}0 & T\geq \mathrm{T}_{liq}\quad (Liquid)\\ \dfrac{T-T_{liq}}{T_{sol}-T_{liq}} & \mathrm{T}_{sol}<T<\mathrm{T}_{liq}\ (Mushy\ \text{regions})\\ 1 & T\leq \mathrm{T}_{sol}\quad (Solid)\end{cases} \tag{2}$$

At each time-step, the solid fraction f_s is updated iteratively according the following approximation

$$f_s^{k+1}\approx f_s^k+\left(\frac{dF}{dT}\right)^k\left(T^{k+1}-F^{-1}\left(f_s^k\right)\right) \tag{3}$$

F is a function of the temperature T. F^{-1} is the inverse function of F.

The boundary conditions at the right and left sides of Fig. 2 are defined by:

$$\begin{cases}\dfrac{\partial T\left(x=L_t,\ \mathrm{t}\right)}{\partial x}=0 & (\text{Right boundary})\\ T\left(x=0,\ \mathrm{t}\right)=T_c & (\text{Left boundary})\end{cases} \tag{4}$$

The initial condition is given by:

$$T(x,\ t{=}0) = 37\ ^{0}\mathrm{C} \tag{5}$$

The one-dimensional *Pennes* bio-heat equation (1) is solved by using a finite-volume method. The scheme adopted for the time discretization is implicit. The resulting set of algebraic equations is then solved by using the Tri-Diagonal-Matrix-Algorithm (TDMA) [30].

The mathematical model accuracy was validated by comparing it to the Neumann's solution. The freezing temperature was set equal to T_c=-196 °C. The metabolic heat generation and blood perfusion rate were set equal to zero. Fig. 3 compares the upper phase change interface position (liquidus temperature T_{liq}) predicted by the present model to the Neumann's solution. The agreement between both solutions is excellent.

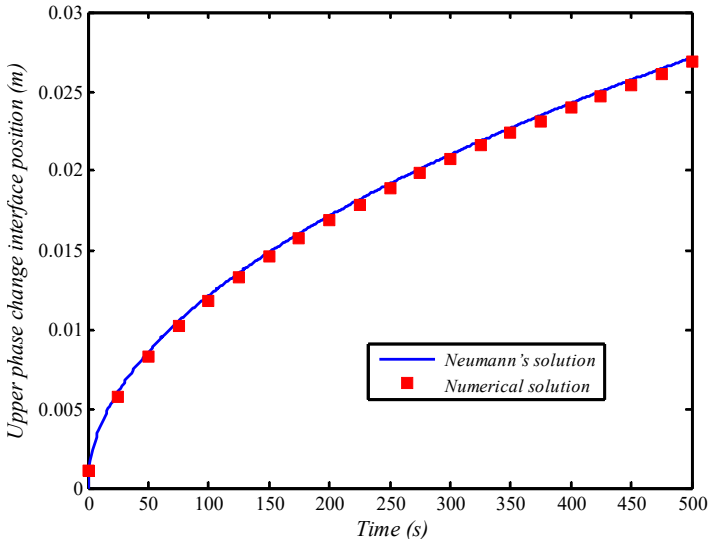

Fig. 3 Comparison of the FVM with Neumann's solution

IV. The Inverse Problem

In the inverse model, it is assumed that (1) the blood perfusion rate w_b and (2) the metabolic heat generation Q_m are unknown. They are estimated from the inverse method and then fed to the direct model that calculates the temperature distributions $T(x,t)$ and the phase change interface position $s(t)$. Therefore, the objective of the inverse method is to determine the unknown coefficients $\vec{P} = \{w_b,\ Q_m\}$ by using temperature measurements taken from a temperature probe pressed against the diseased tissue (Fig. 4).

The estimation of these thermal properties can be constructed as a problem of minimization of the least square norm $\Psi(\vec{P})$

$$\Psi(\vec{P}) = \sum_{i=1}^{I}\left[Y(t_i) - \hat{T}(t_i,\vec{P})\right]^2 \tag{6}$$

where $P = (w_b,\ Q_m)$ is the set of unknown thermal parameters. I is the total number of measurements. $Y(t_i)$ are the temperatures (also called the direct temperatures) measured with the temperature probe. In the present study, these temperatures are 'generated' from the solution of the direct problem wherein the parameters $P = (w_b,\ Q_m)$ are specified. $\hat{T}(t_i,\vec{P})$ are the estimated temperatures from the inverse problem. Thus, the solution of the inverse problem is obtained when the least square norm (6) is minimized.

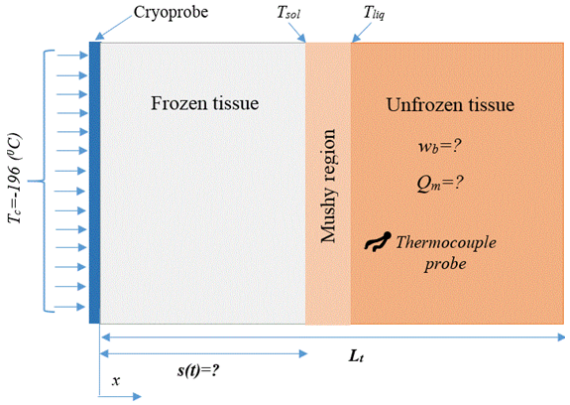

Fig. 4 Inverse problem of cryosurgery. w_b and Q_m are unknown. They are estimated from temperature measurements provided by a temperature probe

The *Levenberg–Marquardt* method is used for the solution of the present inverse problem. This method has been successfully applied to inverse problems in the past [31], [32]. In this iterative method, the incremental value of the unknown parameters ΔP, is written as:

$$\Delta\vec{P}=\left[\left(\vec{J}^{k}\right)^{T}\vec{J}^{k}+\mu^{k}\vec{\Omega}^{k}\right]^{-1}\left(\vec{J}^{k}\right)^{T}\left(\vec{Y}-\vec{T}\left(\vec{P}^{k}\right)\right) \quad (7)$$

μ^{k} is a positive scalar, called the '*damping parameter'*. The choice and the update of this parameter are discussed in [33]. $\vec{\Omega}^{k}=diag\left(\vec{J}^{k}\right)^{T}\vec{J}^{k}$ is a diagonal matrix. $\vec{J}^{k}$ is the '*sensitivity matrix'*, also called the '*Jacobian matrix*'

$$\vec{J}=\begin{pmatrix}\frac{\partial T_1}{\partial w_b} & \frac{\partial T_1}{\partial Q_m}\\ \frac{\partial T_2}{\partial w_b} & \frac{\partial T_2}{\partial Q_m}\\ \vdots & \vdots\\ \frac{\partial T_I}{\partial w_b} & \frac{\partial T_I}{\partial Q_m}\end{pmatrix} \quad (8)$$

The *Jacobian matrix* plays a crucial role in the estimation of the thermal parameters. In fact, there are several approximations for computing the Jacobian matrix [9]. In the current study, the Jacobian matrix is approximated with a finite difference approximation

$$J_{ij}=\frac{\partial\hat{T}_i}{\partial P_j}\cong\frac{\hat{T}\left(t_i;P_1,..,P_j+\left(\delta P_j\right),..P_N\right)-\hat{T}\left(t_i;P_1,..,P_j-\left(\delta P_j\right),..P_N\right)}{2\left(\delta P_j\right)} \quad (9)$$

The subscripts *i* and *j* represent the time and the parameter, respectively. The parameter perturbation $\left(\delta P_j\right)$ is set to $\xi\left(1+\left|P_j\right|\right)$, where ξ is an arbitrary small number.

In order to reduce the computational effort, the Jacobian matrix is updated using the *Broyden* method [34].

$$J_k=J_{k-1}+\frac{\left(\left(\hat{T}_k-\hat{T}_{k-1}\right)-J_{k-1}\Delta P_{k-1}\right)\Delta P_{k-1}^{T}}{\Delta P_{k-1}^{T}\Delta P_{k-1}} \quad (10)$$

$\left(\Delta P_{k-1}\right)$ is the incremental value of the unknown parameters. $\left(\hat{T}\right)$ are the estimated temperatures. Further details about this inverse method are provided in [35]-[38].

The main steps involved in the computational procedure for the direct and the inverse problems are summarized in Figs. 5 and 6, respectively.

V. Results and Discussion

In order to evaluate the temperature distribution *T(x,t)* and the time-varying phase change interface position *s(t)*, the unknown thermal properties of the biological tissue must first be determined. To achieve this task, the above inverse procedure (Fig. 6) was implemented. It predicts simultaneously the metabolic heat generation Q_m and the blood perfusion rate w_b. Once these thermal parameters are obtained, the temperature distribution *T(x,t)* and the time-varying phase change interface position *s(t)* are calculated with the direct model described in Section III.

The freezing temperature was fixed at T_c= -196 °C, and the thickness of tissue was set equal to 0.05 m. The duration of cryosurgery was set equal to *t*= 500 s. The total number of measurements (temperatures recorded by the temperature probe during cryosurgery) is set equal to *I*=50.

All simulations presented here were conducted with a grid space of $dx=2.5*10^{-4}$ *m* and a time step of *dt*=10 *s*. Additional simulations were conducted to make sure that the predictions are grid space and time step independent. All simulations were performed using the MATLAB software running on an Intel@ Core(TM) i5-2520M CPU@ 2.50 GHz.

In order to demonstrate the ability of the inverse method for determining the blood perfusion rate and the metabolic heat generation, two different diseased tissues (lung tumor and breast tumor) were considered. The thermal-physical properties of these diseased tissues are summarized in TABLEI [39]-[41].

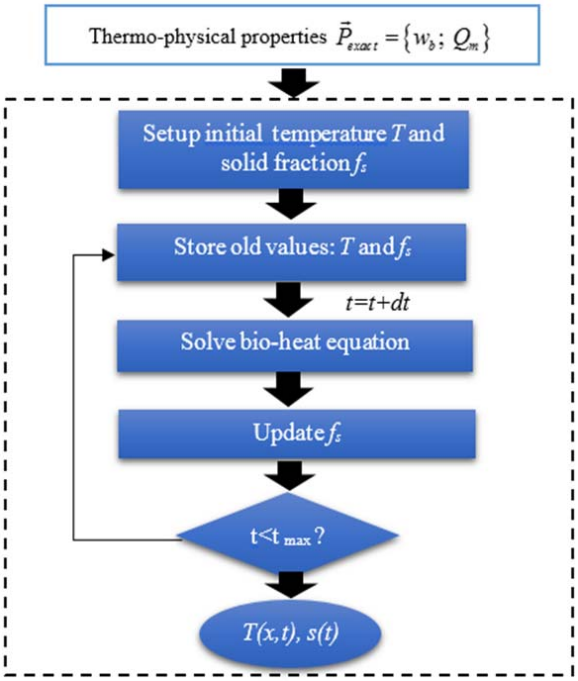

Fig. 5 The direct problem

To characterize the accuracy of the proposed inverse method, two relative errors 'for the blood perfusion rate and the metabolic heat generation' are used. These errors are defined as

$$Error_{w_b}\ (\%)=100\times\left|\frac{w_b^{exact}-w_b^{inverse}}{w_b^{exact}}\right| \quad (11)$$

$$Error_{Q_m}\ (\%)=100\times\left|\frac{Q_m^{exact}-Q_m^{inverse}}{Q_m^{exact}}\right| \quad (12)$$

The superscripts '*exact*' and '*inverse*' refer to the exact solution obtained with the direct model and the inverse

solution predicted by the inverse model, respectively.

TABLE I
THERMO-PHYSICAL PROPERTIES OF TUMORS

	Symbol	Lung tumor	Breast tumor	Unit
Specific heat of unfrozen tumor tissue	c_u	4200	3600	J/kg °C
Specific heat of frozen tumor tissue	c_f	1230	1800	J/kg °C
Thermal conductivity of unfrozen tumor tissue	k_u	0.552	0.51	W/m °C
Thermal conductivity of frozen tumor tissue	k_f	2.23	2	W/m °C
Density of unfrozen tumor tissue	ρ_u	1000	1000	kg/m3
Density of frozen tumor tissue	ρ_f	1000	1000	kg/m3
Lower phase transition temperature	T_{sol}	−8	−8	°C
Upper phase transition temperature	T_{liq}	−1	−1	°C
Latent heat of freezing	L	333	335	kJ/kg
Blood temperature	T_b	37	37	°C
Blood specific heat capacity	c_b	3640	3640	J/kg °C
Blood density	ρ_b	1000	1000	kg/m3
Blood perfusion rate	w_b	**0.002**	**0.009**	ml/s ml
Metabolic heat generation	Q_m	**42000**	**29000**	W/m3

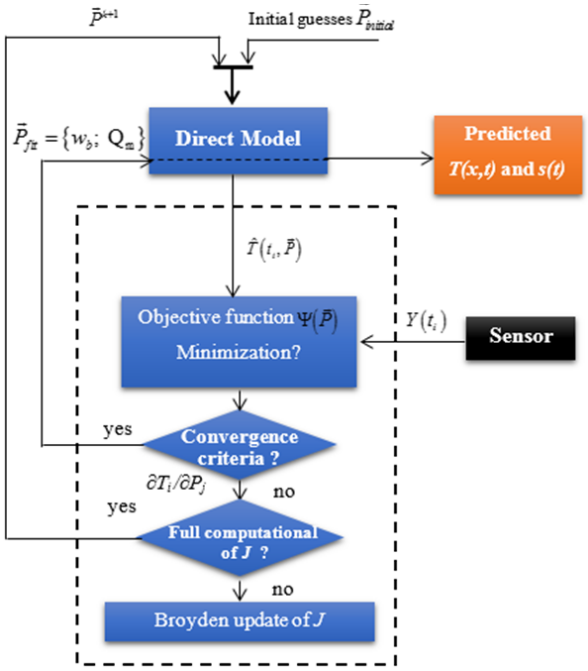

Fig. 6 The inverse problem

The effect of the initial guess values of the blood perfusion rate and of the metabolic heat generation on the convergence of the inverse model is shown in Figs. 7 and 8, respectively. The initial guesses for *test#1, test#2, test#3,* and *test#4* were set equal to 1/3, 1/5, 1/7, and 1/9 of that of the exact value, respectively. It is seen that the convergence of the inverse method is excellent in all cases.

The results of the inverse predictions are summarized in Table II. Examination of this table reveals that the prediction of the blood perfusion rate and of the metabolic heat generation are good for the both tumors. The maximum recorded error is less than 0.7%.

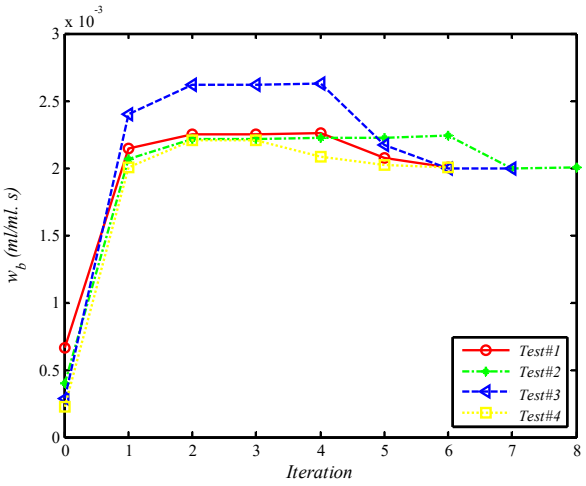

Fig. 7 Convergence of blood perfusion rate (lung tumor)

Fig. 9 compares the exact and the estimated motion of the lower phase change interface *s(t)* during the freezing process for the both tumors. It is seen that the inverse solution (the solution obtained from the inverse model) and the exact solution (the solution provided by the direct model) are in perfect agreement. One may observe that the phase change interface position in the lung tumor gets ahead of the breast tumor. This is due the smaller blood perfusion rate of the lung tumor (0.002 *ml/s.ml*) compared with the breast tumor (0.009 *ml/s.ml*).

TABLE II
INVERSE PREDICTION OF BLOOD PERFUSION AND METABOLIC HEAT GENERATION

	Parameter	P_{Exact}	$P_{Inverse}$	Error%
Lung cancer	w_b	$2*10^{-3}$	$2.0*10^{-3}$	0
	Q_m	$4.2*10^{4}$	$4.18*10^{4}$	0.48
Breast tumor	w_b	$9*10^{-3}$	$9*10^{-3}$	0
	Q_m	$2.9*10^{4}$	$2.88*10^{4}$	0.69

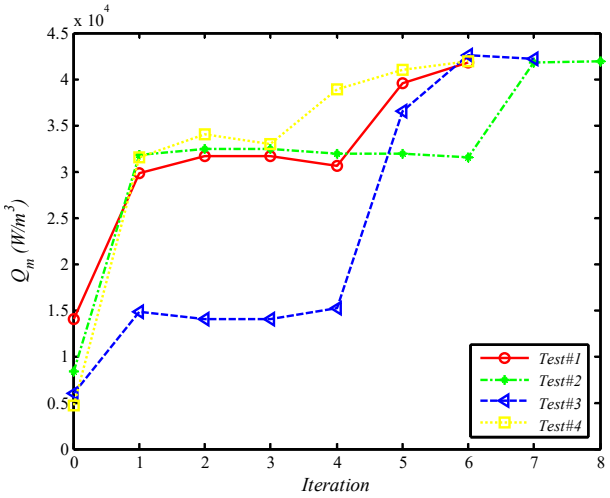

Fig. 8 Convergence of metabolic heat generation (lung tumor)

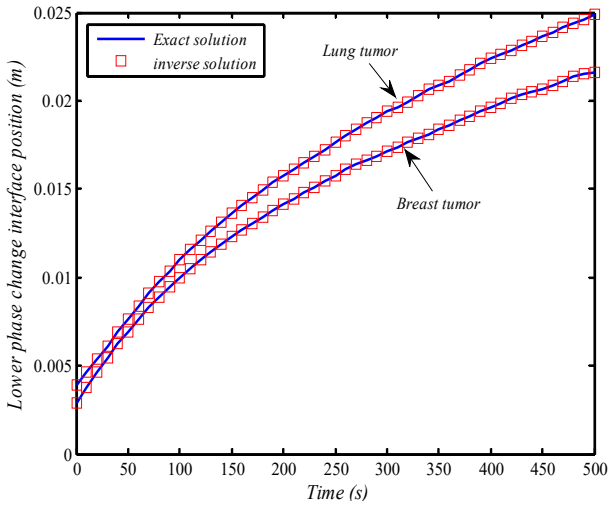

Fig. 9 Lower phase change interface for both tumors

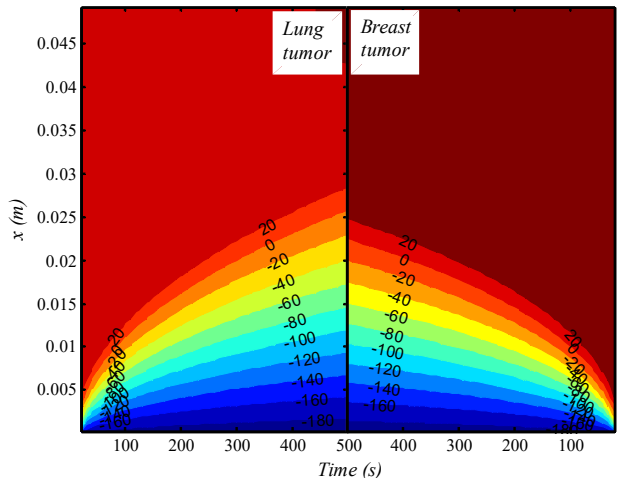

Fig. 10 Temperature distribution for both tumors

The temperature contours predicted with the inverse model for both tumors are also presented in Fig. 10.

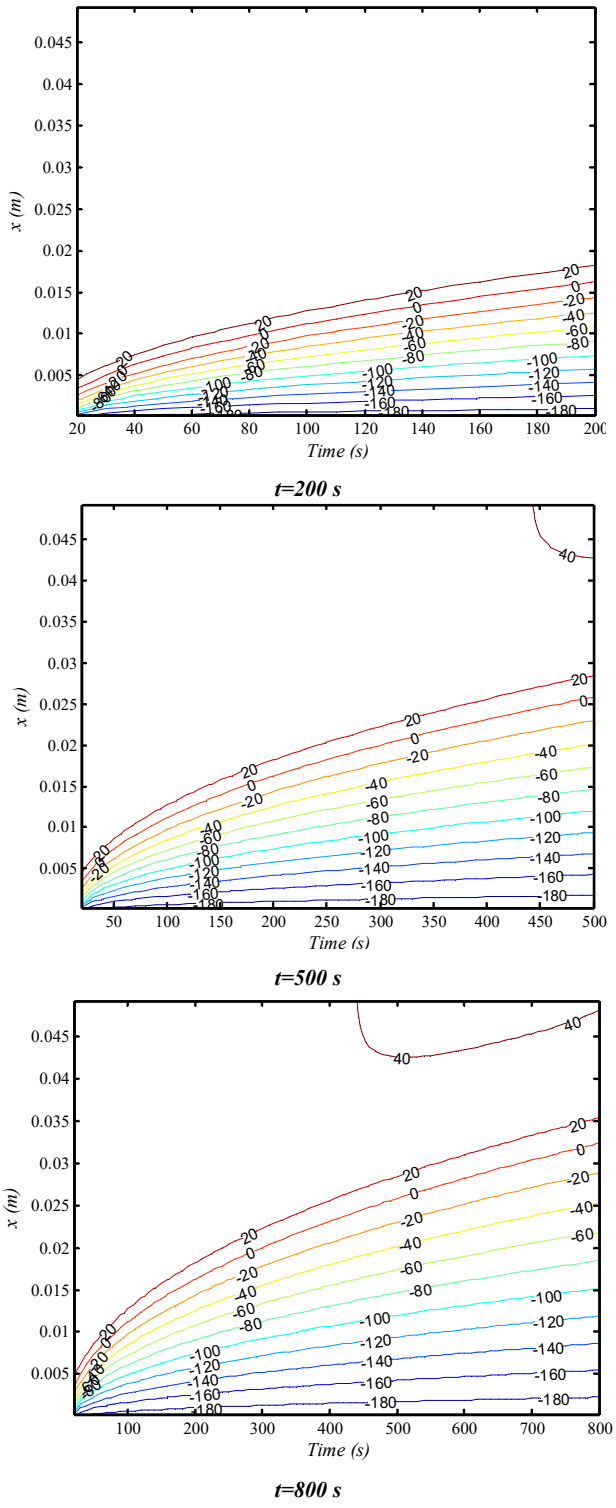

Fig. 11 Effect of cryosurgery duration on temperatures distribution

TABLE III presents the effect of cryosurgery duration on

the inverse predictions. The duration of cryosurgery was set equal to 200, 500, and 800 s. It is seen that the inverse predictions of the metabolic heat generation and of the blood perfusion rate are good for all cases. The relative error recorded is less than 0.5%. The corresponding temperature contours are depicted in Fig. 11. As expected, the freezing region expands with increasing duration of cryosurgery.

TABLE III
EFFECT OF CRYOSURGERY DURATION ON INVERSE PREDICTIONS

Time (s)	*Parameter*	$P_{Inverse}$	*Error%*
200	w_b	$2.0*10^{-3}$	0
	Q_m	$4.198*10^{4}$	0.2
500	w_b	$2.0*10^{-3}$	0
	Q_m	$4.18*10^{4}$	0.4
800	w_b	$2.0*10^{-3}$	0
	Q_m	$4.19*10^{4}$	0.2

A. Effect of Noise on the Inverse Predictions

In this section, the temperatures recorded by the temperature probe were contaminated with measurement errors (or noise) using a random number generator ($randn$) $\vec{\omega}_i$. These measurement errors are added to the recorded temperatures (the exact temperatures $\vec{T}_{exact}$ provided by the direct model):

$$\vec{T}_{\text{noise}}(\text{t}_i) = \vec{T}_{exact}(\text{t}_i) + \sigma\ \vec{\omega}_i \tag{13}$$

σ is the standard deviation of the measurement errors. The value for σ is arbitrarily set equal to *2%* T_{max} and to *4%* T_{max}. T_{max} is the maximum temperature measured by the temperature probe.

Table IV summarizes the effect of the noise and of the total number of measurements I on the inverse predictions. As expected, when the noise level rises from $2\%T_{max}$ to $4\%T_{max}$, the relative errors on the predicted blood perfusion rate and metabolic heat generation increase. Nevertheless, the inverse method remains stable and accurate. On the other hand, when the total number of measurements is increased from *I=50* to *I=100*, the relative errors drop.

TABLE IV
EFFECT OF NOISE AND OF *I* ON THE INVERSE PREDICTIONS

		I=50	*I=100*
σ=0% (no noise)	$Error_{\text{wb}}$	0	0
	$Error_{\text{Qm}}$	0.48	0.23
σ=2%	$Error_{\text{wb}}$	7.11	5.10
	$Error_{\text{Qm}}$	18.05	7.04
σ=4%	$Error_{\text{wb}}$	31.56	5.41
	$Error_{\text{Qm}}$	36.55	18.39

VI. CONCLUSION

This paper presented an inverse heat transfer approach for predicting the time-varying phase change interface and the temperature distribution of diseased tissue during cryosurgery. Using a temperature probe pressed against the layer of diseased tissue, the inverse approach is able to determine simultaneously the metabolic heat generation and the blood perfusion rate. Once these thermal properties are obtained, the temperature distribution and the time-varying phase change interface may be predicted with the direct model. The direct problem is handled with the Pennes bioheat equation and the enthalpy method. The inverse model rests on the *Levenberg-Marquardt* Method (LMM) combined to the *Broyden* Method (BM). The effect (1) of the initial guesses for the unknown thermal properties; (2) of the thermal properties of the diseased tissues; (3) of the data capture frequency; and (4) of the noise on the recorded temperature was investigated. It was shown that the proposed inverse method remains accurate and stable for all the cases investigated.

ACKNOWLEDGMENT

The authors are grateful to the Natural Sciences and Engineering Research Council of Canada (NSERC) for the financial support.

NOMENCLATURE

c	specific heat [J/kg°C]
dt	time step [s]
fs	solid fraction
I	total number of measurements
J	Jacobian matrix
k	thermal conductivity [W/m °C]
L	latent heat of freezing [J/kg]
L_t	thickness of tissue [m]
N	number of unknown parameters
$\vec{P}$	vector of unknown parameter
Q_m	metabolic heat generation[W/m^3]
$Error$	estimation errors [%]
$s(t)$	freezing front position [m]
t	time [s]
$\hat{T}$	estimated temperature [°C]
T_b	arterial blood temperature [°C]
T_c	cryogenic probe temperature [°C]
x	cartesian spatial coordinate [m]
Y	measured temperature [°C]
w_b	blood perfusion rate [$ml/s\ ml$]

A. Greek Symbols

ε	small number
μ	damping parameter
ρ	density of tissue [kg/m^3]
σ	standard deviation of the measurement error
Ψ	sum of squares norm
ξ	small number
δH	enthalpy [J/m^3]
Δ	difference
Ω^k	diagonal matrix
ω	random number

B. Subscripts

b	blood
$exact$	exact solution
f	frozen region
liq	liquidus

max	maximum
u	unfrozen region
P	parameter
sol	solidus
T	temperature

C. Superscripts

k	time iteration number
T	transposed matrix
ˆ	estimated parameter
¯	vector
¨	matrix

REFERENCES

[1] S. O. Pfleiderer, M. G. Freesmeyer, C. Marx, R. Kühne-Heid, A. Schneider and W. A. Kaiser, "Cryotherapy of breast cancer under ultrasound guidance: initial results and limitations," *European radiology,* vol. 12, no. 12, pp. 3009-3014, 2002.

[2] P. E. Huber, J. W. Jenne, R. Rastert, I. Simiantonakis, H. P. Sinn and H. J. Strittmatter, "A new noninvasive approach in breast cancer therapy using magnetic resonance imaging-guided focused ultrasound surgery," *Cancer research,* vol. 61, no. 23, pp. 8441-8447, 2001.

[3] M. Jaeger and M. Carin, "The front-tracking ALE method: application to a model of the freezing of cell suspensions," *Journal of Computational Physics,* vol. 179, no. 2, pp. 704-735, 2002.

[4] M. Carin and M. Jaeger, "Numerical simulation of the interaction of biological cells with an ice front during freezing," *The European Physical Journal Applied Physics,* vol. 16, no. 3, pp. 231-238, 2001.

[5] X. Zhao and K. J. Chua, "Studying the thermal effects of a clinically-extracted vascular tissue during cryo-freezing," *Journal of Thermal Biology,* vol. 37, no. 8, pp. 556-563, 2012.

[6] M. A. Khanday and F. Hussain, "Explicit formula of finite difference method to estimate human peripheral tissue temperatures during exposure to severe cold stress," *Journal of thermal biology,* vol. 48, pp. 51-55, 2015.

[7] G. Delhomme, A. Dittmar, W. H. Newman, H. F. Bowman and M. Jouvet, "Thermal diffusion probes for tissue blood flow measurements," *Sensors and Actuators B: Chemical,* vol. 6, no. 1-3, pp. 87-90, 1992.

[8] M. Burger and F. V. Breukelen, "Construction of a low cost and highly sensitive direct heat calorimeter suitable for estimating metabolic rate in small animals," *Journal of Thermal Biology,* vol. 38, no. 8, pp. 508-512, 2013.

[9] M. N. Ozisik and H. R. B. Orlande, Inverse Heat Transfer, New York: Taylor and Francis, 2000.

[10] H. L. Lee, T. H. Lai, W. L. Chen and Y. C. Yang, "An inverse hyperbolic heat conduction problem in estimating surface heat flux of a living skin tissue," *Applied Mathematical Modelling,* vol. 37, no. 5, pp. 2630-2643, 2013.

[11] H. L. Lee, T. H. Lai, W. L. Chen and Y. C. Yang, "An inverse hyperbolic heat conduction problem in estimating surface heat flux of a living skin tissue," *Applied Mathematical Modelling,* vol. 37, no. 5, pp. 2630-2643, 2013.

[12] K. Das, R. Singh and S. C. Mishra, "Numerical analysis for determination of the presence of a tumor and estimation of its size and location in a tissue," *Journal of thermal biology,* vol. 38, no. 1, pp. 32-40, 2013.

[13] R. Das, S. C. Mishra and R. Uppaluri, "Multiparameter estimation in a transient conduction-radiation problem using the lattice Boltzmann method and the finite-volume method coupled with the genetic algorithms," *Numerical Heat Transfer,* vol. 53, no. 12, pp. 1321-1338, 2008.

[14] P. W. Partridge and L. C. Wrobel, "An inverse geometry problem for the localisation of skin tumours by thermal analysis," *Engineering Analysis with Boundary Elements,* vol. 31, no. 10, pp. 803-811, 2007.

[15] K. Das and S. C. Mishra, "Non-invasive estimation of size and location of a tumor in a human breast using a curve fitting technique," *International Communications in Heat and Mass Transfer,* vol. 56, pp. 63-70, 2014.

[16] K. Das and S. C. Mishra, "Simultaneous estimation of size, radial and angular locations of a malignant tumor in a 3-D human breast–A numerical study," *Journal of thermal biology,* vol. 52, pp. 147-156, 2015.

[17] J. M. Luna, R. Romero-Mendez, A. Hernandez-Guerrero and F. Elizalde-Blancas, "Procedure to estimate thermophysical and geometrical parameters of embedded cancerous lesions using thermography," *Journal of biomechanical engineering,* vol. 134, no. 3, p. 031008, 2012.

[18] K. Yue, X. Zhang and F. Yu, "Simultaneous estimation of thermal properties of living tissue using noninvasive method," *International Journal of Thermophysics,* vol. 28, no. 5, pp. 1470-1489, 2007.

[19] G. P. Flach and M. N. Özişik, "Inverse heat conduction problem of simultaneously estimating spatially varying thermal conductivity and heat capacity per unit volume," *Numerical Heat Transfer,* vol. 16, no. 2, pp. 249-266, 1989.

[20] C. H. Huang and C. Y. Huang, "An inverse biotechnology problem in estimating the optical diffusion and absorption coefficients of tissue," *International journal of heat and mass transfer,* vol. 47, no. 3, pp. 447-457, 2004.

[21] A. Jalali, M. B. Ayani and M. Baghban, "Simultaneous estimation of controllable parameters in a living tissue during thermal therapy," *Journal of thermal biology,* vol. 45, pp. 37-42, 2014.

[22] Y. T. Zhang and J. Liu, "Numerical study on three-region thawing problem during cryosurgical re-warming," *Medical engineering & physics,* vol. 24, no. 4, pp. 265-277, 2002.

[23] Y. Rabin and A. Shitzer, "Exact solution to the one-dimensional inverse-Stefan problem in non-ideal biological tissues," *Journal of Heat Transfer,* vol. 117, no. 2, pp. 425-431, 1995.

[24] K. J. Chua and S. K. Chou, "On the study of the freeze–thaw thermal process of a biological system," *Applied Thermal Engineering,* vol. 29, no. 17, pp. 3696-3709, 2009.

[25] H. Budman, A. Shitzer and J. Dayan, "Analysis of the inverse problem of freezing and thawing of a binary solution during cryosurgical processes," *Journal of biomechanical engineering,* vol. 117, no. 2, pp. 193-202, 1995.

[26] K. J. Chua, S. K. Chou and J. C. Ho, "An analytical study on the thermal effects of cryosurgery on selective cell destruction," *Journal of biomechanics,* vol. 40, no. 1, pp. 100-116, 2007.

[27] E. H. Wissler, "Pennes' 1948 paper revisited," *Journal of Applied Physiology,* vol. 85, no. 1, pp. 35-41, 1998.

[28] T. L. Horng, T. L. Horng, W. L. Lin, C. T. Liauh and T. C. Shih, "Effects of pulsatile blood flow in large vessels on thermal dose distribution during thermal therapy," *Medical physics,* vol. 34, no. 4, pp. 1312-1320, 2007.

[29] H. H. Pennes, "Analysis of tissue and arterial blood temperatures in the resting human forearm," *Journal of applied physiology,* vol. 1, no. 2, pp. 93-122, 1948.

[30] S. Patankar, Numerical heat transfer and fluid flow, CRC press, 1980.

[31] C. H. Huang and C. Y. Huang, "An inverse problem in estimating simultaneously the effective thermal conductivity and volumetric heat capacity of biological tissue," *Applied mathematical modelling,* vol. 31, no. 9, pp. 1785-1797, 2007.

[32] J. Iljaž and L. Škerget, "Blood perfusion estimation in heterogeneous tissue using BEM based algorithm," *Engineering Analysis with Boundary Elements,* Vols. 75-87, p. 39, 2014.

[33] D. W. Marquardt, "An algorithm for least-squares estimation of nonlinear parameters," *Journal of the society for Industrial and Applied Mathematics,* vol. 11, no. 2, pp. 431-441, 1963.

[34] C. G. Broyden, "A class of methods for solving nonlinear simultaneous equations," *Mathematics of computation,* pp. 577-593, 1965.

[35] M. Hafid and M. Lacroix, "An inverse heat transfer method for predicting the thermal characteristics of a molten material reactor," *Applied Thermal Engineering,* vol. 108, p. 140–149, 2016.

[36] M. Hafid and M. Lacroix, "Inverse Heat Transfer Analysis of a Melting Furnace Using Levenberg-Marquardt Method," *Int. J. of Mechanical, Aerospace, Industrial, Mechatronic and Manufacturing Engineering,* vol. 10, no. 7, pp. 1228-1235, 2016.

[37] M. Hafid and M. Lacroix, "Prediction of the Thermal Parameters of a High-Temperature Metallurgical Reactor Using Inverse Heat Transfer," *Int. J. of Mechanical, Aerospace, Industrial, Mechatronic and Manufacturing Engineering,* vol. 10, no. 6, pp. 907-913, 2016.

[38] M. Hafid and M. Lacroix, "Inverse heat transfer prediction of the state of the brick wall of a melting furnace," *Applied Thermal Engineering,* Vols. 265-274, p. 110, 2017.

[39] S. Kumar and V. K. Katiyar, "Numerical study on phase change heat transfer during combined hyperthermia and cryosurgical treatment of lung cancer," *International Journal of Applied Mathematics and*

Mechanics, vol. 3, no. 3, pp. 1-17, 2007.
[40] A. Zhang, L. X. Xu, G. A. Sandison and J. Zhang, "A microscale model for prediction of breast cancer cell damage during cryosurgery," *Cryobiology,* vol. 47, no. 2, pp. 143-154, 2003.
[41] F. J. González, "Thermal simulation of breast tumors," *Revista mexicana de física,* vol. 53, no. 4, pp. 323-326, 2007.